12-5-2023

Deletion of V**β**3

Cheng Ye

Sadie A Clements

Weihong Gu

Aron M Geurts

Clayton E Mathews

See next page for additional authors

Follow this and additional works at: https://mouseion.jax.org/stfb2023

Original Citation

Ye C, Clements S, Gu W, Geurts A, Mathews C, Serreze DV, Chen Y, Driver J. Deletion of Vβ3 Proc Natl Acad Sci U S A. 2023;120(49):e2312039120.

Authors

Cheng Ye, Sadie A Clements, Weihong Gu, Aron M Geurts, Clayton E Mathews, David V. Serreze, Yi-Guang Chen, and John P Driver

Deletion of Vβ3+CD4+ T cells by endogenous mouse mammary tumor virus 3 prevents type 1 diabetes induction by autoreactive CD8+ T cells

Cheng Ye[a,1], Sadie A. Clements[b,1], Weihong Gu[b], Aron M. Geurts[c], Clayton E. Mathews[d], David. V. Serreze[e] [ID], Yi-Guang Chen[f], and John P. Driver[b,2] [ID]

In both humans and NOD mice, type 1 diabetes (T1D) develops from the autoimmune destruction of pancreatic beta cells by T cells. Interactions between both helper CD4+ and cytotoxic CD8+ T cells are essential for T1D development in NOD mice. Previous work has indicated that pathogenic T cells arise from deleterious interactions between relatively common genes which regulate aspects of T cell activation/effector function (*Ctla4, Tnfrsf9, Il2/Il21*), peptide presentation (*H2-A^{g7}, B2m*), and T cell receptor (TCR) signaling (*Ptpn22*). Here, we used a combination of subcongenic mapping and a CRISPR/Cas9 screen to identify the NOD-encoded mammary tumor virus (*Mtv*)3 provirus as a genetic element affecting CD4+/CD8+ T cell interactions through an additional mechanism, altering the TCR repertoire. *Mtv3* encodes a superantigen (SAg) that deletes the majority of Vβ3+ thymocytes in NOD mice. Ablating *Mtv3* and restoring Vβ3+ T cells has no effect on spontaneous T1D development in NOD mice. However, transferring *Mtv3* to C57BL/6 (B6) mice congenic for the NOD *H2^{g7}* MHC haplotype (B6.*H2^{g7}*) completely blocks their normal susceptibility to T1D mediated by transferred CD8+ T cells transgenically expressing AI4 or NY8.3 TCRs. The entire genetic effect is manifested by Vβ3+CD4+ T cells, which unless deleted by *Mtv3*, accumulate in insulitic lesions triggering in B6 background mice the pathogenic activation of diabetogenic CD8+ T cells. Our findings provide evidence that endogenous *Mtv* SAgs can influence autoimmune responses. Furthermore, since most common mouse strains have gaps in their TCR Vβ repertoire due to *Mtvs*, it raises questions about the role of *Mtvs* in other mouse models designed to reflect human immune disorders.

type 1 diabetes | endogenous retrovirus | Mtv3 | thymic deletion

Type 1 diabetes (T1D) is a polygenic autoimmune disease with over 50 genetic linkages identified in both rodents and humans (1). A preponderance of evidence supports that both CD4+ and CD8+ T cells act as final effectors of pancreatic beta-cell death. This includes that autoimmune responses of CD4+ and CD8+ T cells have been measured to over 15 distinct antigens in T1D patients as well as against 8 antigens in T1D-prone NOD mice (2, 3). In both humans and mice, a single locus containing the major histocompatibility complex (MHC) genes is the primary disease risk factor. However, generation of pathogenic T cells also requires interactive contributions from a variety of non-MHC genes, including those encoding T cell–directed cytokines and cytokine receptors, positive and negative regulators of the TCR (T cell receptor) signaling cascade, and T cell costimulatory/inhibitory molecules (1).

The possibility that endogenous retroviruses are involved in the genetic etiology of T1D has been the subject of much debate (4). Studies in the 1990s suggested that viral superantigens (SAgs) encoded within mammary tumor viruses (*Mtv*s) in NOD mice (5) and IDDMK(1,2)22 (6–8), a closely related human endogenous retrovirus (HERV), provoke T1D by activating T cells that cross-react with islet antigens. Although these findings generated controversy (9–11), subsequent studies showed that two HERVs, HERV-W and HERV-K, are abnormally expressed in humans with T1D. An envelope protein encoded by HERV-W, also associated with multiple sclerosis lesions, has been found localized to pancreatic lesions of T1D patients where it spreads in parallel with disease progression (12). In contrast, a low number of HERV-K(C4) copies in the complement 4 gene cluster has been linked to an increased risk of T1D (13), indicating that endogenous retroviral insertions may play a protective role in disease. Additionally, HERV-K18 on human Chromosome (Chr.) 1 encodes a SAg which has been reported to be capable of deleting Vβ7 CD4+ T cells in human thymi, in a similar way to *Mtv* SAgs (14). While these and more recent studies (15, 16) suggest that endogenous retrovirus-encoded antigens may have a considerably greater influence on human immune responses than once appreciated, understanding the mechanism through which they

Significance

Several common pathogenic viruses have been associated with the onset of type 1 diabetes (T1D). This has led to a proposed role for viral antigens and/or viral superantigens (SAgs) in eliciting activation of T cells that react with self-antigens, resulting in the initiation of autoimmunity in genetically susceptible individuals. We identified mouse mammary tumor provirus (*Mtv*)3 as underlying insulin-dependent diabetes 32 (*Idd32*) diabetes resistance locus in the T1D susceptible NOD mouse, the primary animal model for studying human T1D. The mechanism of protection is via *Mtv3* SAg-mediated alteration in the collaboration between CD4+ and CD8+ T cells, which is essential for T1D development. Our results support that proviral SAgs may influence T1D and other immune diseases in genetically susceptible humans.

function is complicated by the genetic heterogeneity that exists among humans, especially in terms of the diversity of MHC molecules with which HERVs interact. The current work indicates that inbred mice with their ~30 well-defined endogenous *Mtvs*, including detailed information on how individual SAgs modulate the T cell repertoire in the context of different MHC haplotypes (17), can offer unique insights into how retroviral SAgs interact with the immune system, which could benefit a number of human diseases.

NOD mice are considered a valid model of human T1D due partly to similarities in loci and genes and the biochemical networks in which they function that confer susceptibility to autoimmunity. Outcrosses of NOD mice to nominally resistant strains have uncovered that the NOD genome also harbors latent T1D resistance genes which are normally masked by the large number of disease susceptibility alleles this strain carries (18–24). This includes a dominantly acting T1D inhibitor in the distal region of Chr. 11 (25). This finding was based on the observation that adoptively transferred CD8$^+$ T cells transgenically expressing the diabetogenic AI4 TCR rapidly induced T1D in both sublethally irradiated NOD mice and C57BL6/J (B6) mice congenic for the NOD derived $H2^{g7}$ MHC haplotype (B6.$H2^{g7}$) but failed to transfer disease or significant levels of insulitis to (NOD × B6.$H2^{g7}$)F1 (F1) hybrids (25). F1 hybrid resistance indicated that the NOD and B6.$H2^{g7}$ genomes harbor separate recessively acting alleles that promote the activation of pathogenic CD8$^+$ T cells. Alleles of B6 origin were identified by performing a SNP-based genome-wide scan analysis of AI4-injected progeny derived from a first backcross (BC1) of (NOD × B6.$H2^{g7}$)F1 hybrids to the B6.$H2^{g7}$ parental strain. This revealed a single B6-derived recessive locus on Chr.11 as highly associated with susceptibility to AI4 T cell–induced T1D and insulitis (logarithm of odds score = 13.2). The genomic region of interest, designated as insulin-dependent diabetes locus 32 (*Idd32*), was narrowed to a ~8-Mb interval from 113.98 Mb to the end of Chr.11 (121.8 Mb) containing more than 270 genes.

The current study describes how we used a combination of congenic truncation mapping and a CRISPR/Cas9 gene targeting strategy, which enables candidate gene testing by allele-specific expression, to identify mouse *Mtv3* as the genetic element underlying *Idd32*. Like other endogenous mouse *Mtvs*, *Mtv3* encodes a type II transmembrane glycoprotein SAg that interacts with MHC class II molecules and binds to the variable domain of specific TCR Vβ chains (26, 27). When presented as a self-antigen in the thymus, SAgs induce the Vβ-specific deletion of SAg-reactive T cells, the specificity of which is determined by polymorphisms within the carboxy terminus region of individual SAgs (28, 29). Our results indicate that the *Mtv3* SAg carried by NOD mice eliminates precursors of Vβ3$^+$ T cells which were found to be the sole drivers of peripheral autoreactive CD8$^+$ T cell activation in normally T1D-resistant B6.$H2^{g7}$ mice. These findings may reinvigorate the debate about whether the presence or absence of HERV elements contributes to T1D pathogenesis and other human diseases.

Results

NOD and B6 Alleles at *Idd32* Differentially Control Diabetogenic CD8$^+$ T Cells through CD4$^+$ T Cells. We previously found that sublethally irradiated (NOD × B6.$H2^{g7}$)F1 × B6.$H2^{g7}$ BC1 mice homozygous vs. heterozygous for B6 alleles at *Idd32*, in tight linkage with microsatellite marker *D11Mit48*, were, respectively, highly susceptible and resistant to AI4-induced diabetes and insulitis (25). AI4 is a beta cell cytotoxic CD8$^+$ T cell clone originally isolated from the islet infiltrate of a 5 to 6-wk-old prediabetic female NOD mouse that recognizes a peptide from the insulin A chain (30). A series of adoptive transfer studies determined that the genetic effect
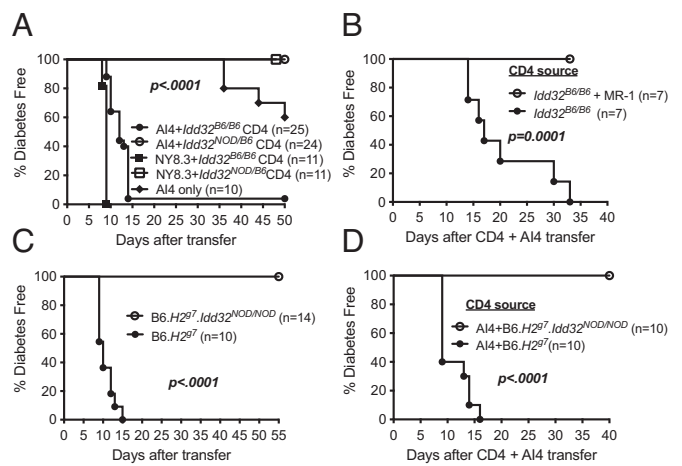

Fig. 1. A polymorphic gene in close linkage with the marker *D11Mit48* controls susceptibility to diabetogenic CD8$^+$ T cell–induced T1D through effects on a CD4$^+$ T cell population. (*A*) Incidence of T1D in B6.$H2^{g7}$.*Rag1^{null}* recipients of 1 × 10^7 NOD.*Rag1^{null}*.*AI4* splenocytes or 1 × 10^6 NY8.3 CD8$^+$ T cells coinfused with 2 × 10^6 purified CD4$^+$ T cells from *Idd32$^{B6/B6}$* or *Idd32$^{NOD/B6}$* BC1 segregants. (*B*) Diabetogenic *Idd32$^{B6/B6}$* BC1 CD4$^+$ T cells require CD40-CD40L interactions to pathogenically activate AI4 T cells. Incidence of T1D in B6.$H2^{g7}$.*Rag1^{null}* recipients receiving 1 × 10^7 NOD.*Rag1^{null}*.*AI4* splenocytes and 2 × 10^6 purified CD4$^+$ T cells from *Idd32$^{B6/B6}$* BC1 segregants and treated with 0.5 mg anti-CD154 blocking antibody (MR-1) or rat IgG control every 4 d. (*C*) After sublethal irradiation, B6.$H2^{g7}$ mice or B6.$H2^{g7}$ mice congenically expressing NOD alleles at *D11Mit48* (B6.$H2^{g7}$.*Idd32$^{NOD/NOD}$*) were, respectively, highly susceptible and highly resistant to T1D induced by subsequent infusion with 1 × 10^7 AI4 splenocytes. (*D*) T1D incidence for B6.$H2^{g7}$.*Rag1^{null}* mice injected with 2 × 10^6 purified CD4$^+$ T cells from B6.$H2^{g7}$ or B6.$H2^{g7}$.*Idd32$^{NOD/NOD}$* mice with 1 × 10^7 NOD.*Rag1^{null}*.*AI4* splenocytes. Survival curves were compared by the log-rank test.

is manifested by host CD4$^+$ T cells. When total CD4$^+$ T cells from *D11Mit48$^{B6/B6}$* (*Idd32$^{B6/B6}$*) or *D11Mit48$^{NOD/B6}$* (*Idd32$^{NOD/B6}$*) BC1 progeny are cotransferred with NOD.*Rag1^{null}*.*AI4* splenocytes into B6.$H2^{g7}$.*Rag1^{null}* mice, only recipients cotransferred with CD4$^+$ T cells from *Idd32$^{B6/B6}$* homozygous but not *Idd32$^{NOD/B6}$* heterozygous BC1 donors develop T1D and high levels of insulitis [Fig. 1*A* and (25)]. We further identified that *Idd32$^{B6/B6}$* CD4$^+$ T cells require CD40-CD40L interactions to pathogenically activate AI4 T cells. This was demonstrated by the finding anti-CD40L antibody administration prevents T1D in B6.$H2^{g7}$.*Rag1^{null}* mice injected with *Idd32$^{B6/B6}$* CD4$^+$ T cells and NOD.*Rag1^{null}*.*AI4* splenocytes (Fig. 1*B*). To determine whether *Idd32* allelic differences within CD4$^+$ T cells are sufficient to control the pathogenic activation of an autoreactive CD8$^+$ T cell clonotype recognizing a different autoantigen, the above experiment was repeated using islet-specific glucose-6-phosphate catalytic subunit-related protein-reactive CD8$^+$ T cells purified from NOD.*NY8.3* mice in place of NOD.*Rag1^{null}*.*AI4* splenocytes. Again, T1D was induced in *Idd32$^{B6/B6}$* but not in *Idd32$^{NOD/B6}$* CD4$^+$ T cell–harboring recipients (Fig. 1*A*).

To further delineate the *Idd32* locus and eliminate the possibility that genes outside the interval contribute to CD8$^+$ T cell–induced T1D susceptibility, we generated a congenic stock of B6.$H2^{g7}$ mice homozygous for the NOD allele of *D11Mit48* (B6.$H2^{g7}$.*Idd32$^{NOD/NOD}$*). Sublethally irradiated B6.$H2^{g7}$ and B6.$H2^{g7}$.*Idd32$^{NOD/NOD}$* mice were respectively entirely susceptible and highly resistant to AI4-induced T1D (Fig. 1*C*). Furthermore, CD4$^+$ T cells purified from B6.$H2^{g7}$ and B6.$H2^{g7}$.*Idd32$^{NOD/NOD}$* mice respectively supported and suppressed T1D when adoptively transferred into B6.$H2^{g7}$.*Rag1^{null}* recipients with AI4 T cells (Fig. 1*D*).

***Idd32* Modulates the Activation and Proliferation of CD4$^+$ T Cells and Pathogenic CD8$^+$ T Cell Activation.** To examine how *Idd32* region genes extrinsically modulate diabetogenic CD8$^+$

T cell activation in vivo, we analyzed AI4 T cells in pancreatic lymph nodes (PLN) at 4 d and the spleen at 9 d after their adoptive transfer into sublethally irradiated B6.$H2^{g7}$ and B6.$H2^{g7}$.

$Idd32^{NOD/NOD}$ mice. AI4 T cells recovered from B6.$H2^{g7}$ and B6.$H2^{g7}$.$Idd32^{NOD/NOD}$ mice exhibited phenotypes respectively consistent with highly activated and naïve T cells (Fig. 2 *A–C*).
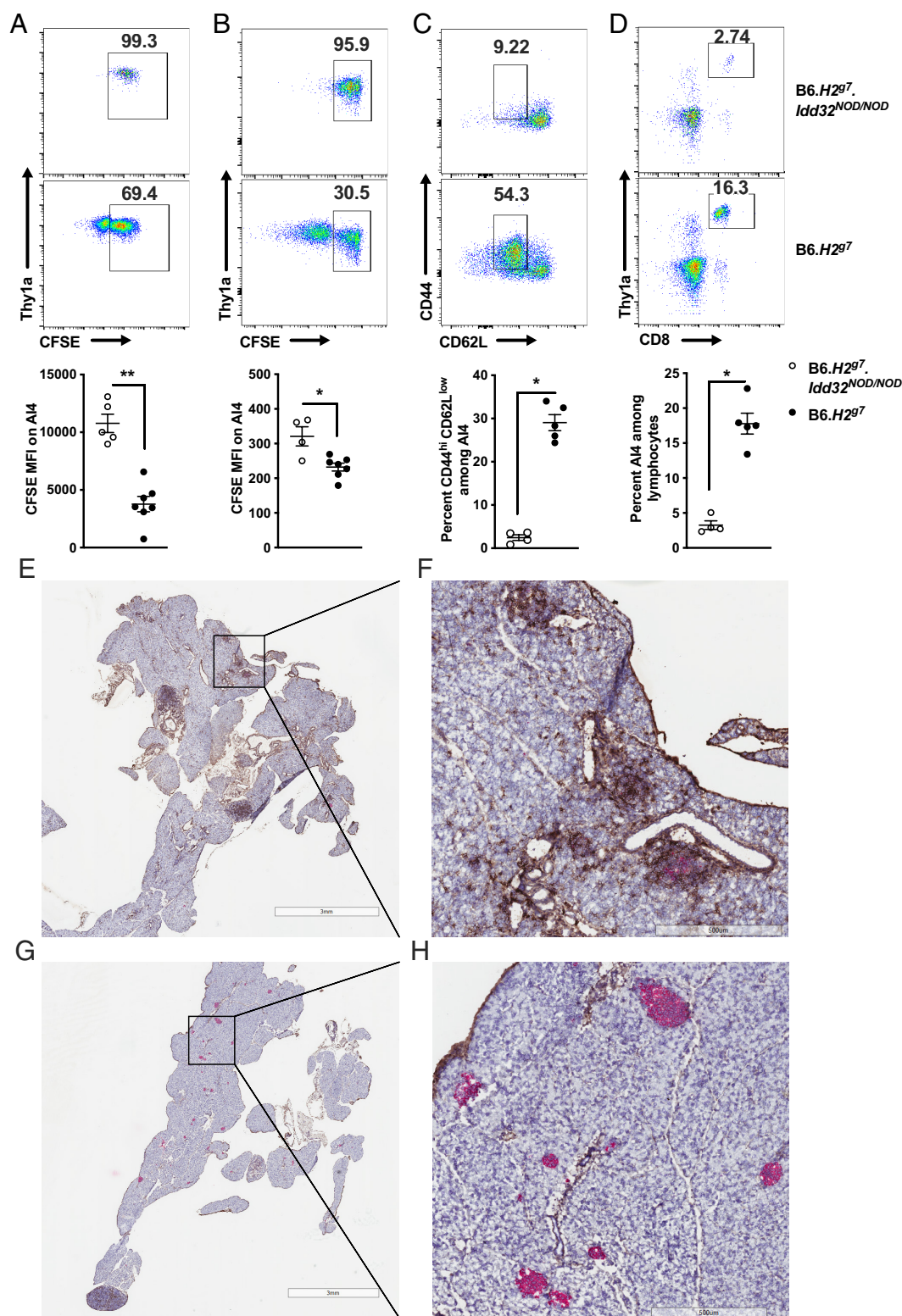

Fig. 2. Pathogenic CD8⁺ T cell activation is differentially affected by B6- and NOD-derived alleles at *Idd32*. Flow cytometry was used to analyze CFSE-labeled Th1a⁺ AI4 T cells in PLN, splenocytes, and PBL of sublethally irradiated B6.$H2^{g7}$ (n = 7) and B6.$H2^{g7}$.$Idd32^{NOD/NOD}$ (n = 4) mice 4 to 9 d after adoptive transfer. (*A* and *B*) In vivo proliferation of CFSE-labeled AI4 T cells in PLN (*A*) and splenocytes (*B*). (*C*) Frequency of activated (CD44⁺CD62L⁻) AI4 T cells in the spleen. (*D*) Frequency of AI4 T cells in PBL. *$*P < 0.05$ and **$*P < 0.005$. (*E–H*) Immunohistochemistry was used to assess insulitis at 10 d post-adoptive transfer. Pancreata were stained for insulin (red) and Thy1a (brown). Little insulin staining and widespread Thy1a staining were observed in B6.$H2^{g7}$ pancreata (*E* and *F*). Significant insulin staining and little Thy1a staining were observed in B6.$H2^{g7}$.$Idd32^{NOD/NOD}$ pancreata (*G* and *H*). Images are longitudinal sections of pancreata at 20× (*E* and *G*) and 200× (*F* and *H*) magnification.
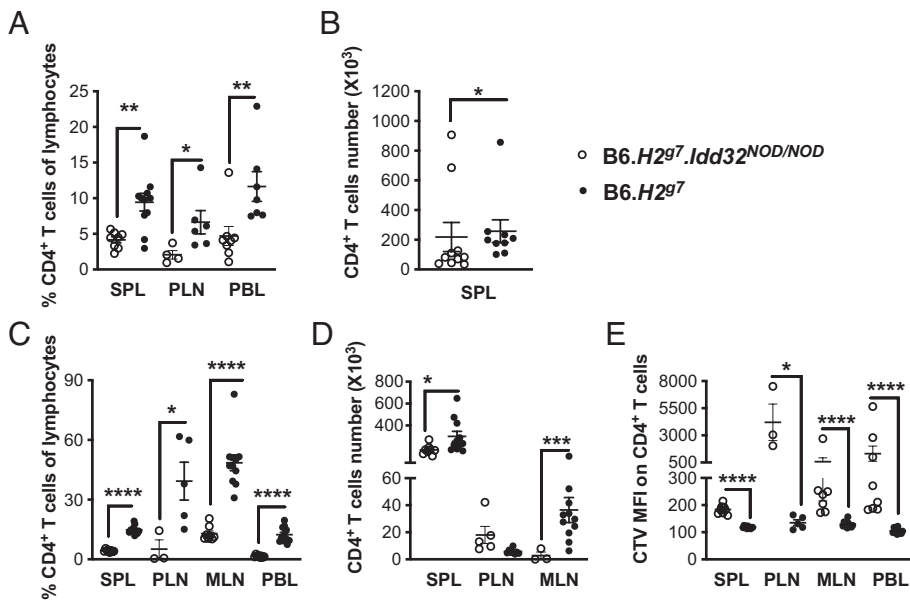
Fig. 3. *Idd32* modulates the activation and proliferation of CD4^{+} T cells. (*A* and *B*) CD4^{+} T cells were analyzed in the spleen, PLN, and PBL of 7- to 10-wk-old female NOD.*Rag1^null* mice 5 d after adoptive transfer with 2×10^6 CD4^{+} T cells from B6.*H2^{g7}*.*Idd32^{NOD/NOD}* or B6.*H2^{g7}* mice and 1×10^7 AI4 T cells. (*A*) The frequency CD4^{+} T cells in the spleen, PLN, and PBL. (*B*) The number of CD4^{+} T cells in the spleen. (*C*–*E*) CTV-labeled CD4^{+} T cells analyzed in the spleen, PLN, mesenteric lymph nodes (MLN), and PBL of 7- to 10-wk-old female NOD.*Rag1^null* mice 5 d after adoptive transfer with 2×10^6 CD4^{+} T cells from B6.*H2^{g7}* and B6.*H2^{g7}*.*Idd32^{NOD/NOD}* mice without AI4 T cells. The frequency (*C*) and number (*D*) of CD4^{+} T cells in the spleen, PLN, MLN, and PBL. (*E*) Proliferation of CD4^{+} T cells in the spleen, PLN, MLN and PBL. Each symbol represents a single mouse. Results are displayed as mean ± SEM and were analyzed by the Mann–Whitney test. *$P < 0.05$, **$P < 0.01$, and ***$P < 0.001$.

Moreover, much higher peripheral blood (PBL) concentrations of AI4 T cells were found in B6.*H2^{g7}* than B6.*H2^{g7}*.*Idd32^{NOD/NOD}* mice (Fig. 2*D*). When immunohistochemistry was used to assess insulitis at 10 d post-adoptive transfer, we found large numbers of AI4 T cells and very few insulin-positive cells in pancreata from B6.*H2^{g7}* mice (Fig. 2 *E* and *F*). In contrast, pancreata from B6.*H2^{g7}*.*Idd32^{NOD/NOD}* mice had very few AI4 T cells (Fig. 2 *G* and *H*).

Next, we addressed how *Idd32* might modulate the activation of CD4^{+} T cells in a coadoptive transfer setting with AI4 CD8^{+} T cells. In this study, recipient mice were analyzed 5 d post-adoptive transfer. Following coengraftment with AI4 T cells there were significantly higher levels in the PBL, PLN, and spleen of B6.*H2^{g7}* than B6.*H2^{g7}*.*Idd32^{NOD/NOD}* CD4^{+} T cells in NOD.*Rag1^null* recipients (Fig. 3 *A* and *B*). It was subsequently determined whether the expansion of B6.*H2^{g7}* CD4^{+} T cells was dependent on the cotransfer of diabetogenic CD8^{+} T cells. To address this question, a cohort of NOD.*Rag1^null* recipients was injected with CTV membrane labeled B6.*H2^{g7}* or B6.*H2^{g7}*.*Idd32^{NOD/NOD}* CD4^{+} T cells in the absence of AI4 T cells. Again, there were significantly higher engraftment levels in NOD.*Rag1^null* recipients of B6.*H2^{g7}* than B6.*H2^{g7}*.*Idd32^{NOD/NOD}* CD4^{+} T cells (Fig. 3 *C* and *D*). Moreover, in all tissues examined, there was greater proliferation of B6.*H2^{g7}* than B6.*H2^{g7}*.*Idd32^{NOD/NOD}* CD4^{+} T cells (Fig. 3*E*). Together, these results suggest that the *Idd32* locus controls the pathogenic activation of diabetogenic CD8^{+} T cells through modulating the activation and proliferation of CD4^{+} T cells.

T1D Development in B6.*H2^{g7}* Mice Congenic for Various Intervals of NOD *Idd32*. To reduce the number of potential gene candidates within the *Idd32* support interval, we generated 9 B6.*H2^{g7}* subcongenic stocks expressing different NOD-derived segments of the original *Idd32* interval (Fig. 4). This was accomplished by backcrossing B6.*H2^{g7}* mice heterozygous for the full-length *Idd32* locus (B6.*H2^{g7}*.*Idd32^{NOD/B6}*) to B6.*H2^{g7}* mice as outlined in the *Materials and Methods*. All recipients of subcongenic lines 1, 2, 3, 8, and 9 developed T1D after injection with NOD.*Rag1^null*. AI4 splenocytes, while subcongenic lines 4-7 were disease resistant (Fig. 4). These results shortened the *Idd32* support interval to a <490-kb region on Chr. 11, between 116.33 and 116.82 Mb. The reduced *Idd32* support interval included 15 protein coding and 4 predicted genes containing NOD/B6 polymorphisms, insertions and deletions, and structural variants (https://www.sanger.ac.uk/data/mouse-genomes-project/) (Table 1).

Allele-Specific Targeting of Candidate Genes. To identify the gene underlying *Idd32* we used a CRISPR/Cas9 screen that allows the selective expression of only the B6 or both the B6 and
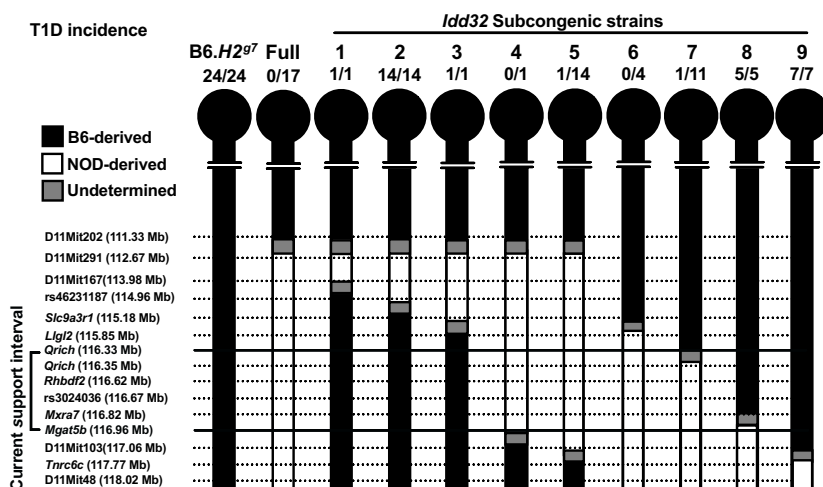
Fig. 4. Comparison of T1D incidence among standard B6.*H2^{g7}* mice vs. B6.*H2^{g7}* strains expressing the full-length interval (Full) or subcongenic segments of the NOD-derived *Idd32* region. AI4 splenocytes were adoptively transferred into sublethally irradiated B6.*H2^{g7}* mice or nine B6.*H2^{g7}* subcongenic stocks expressing different NOD-derived segments of the original *Idd32* interval that were monitored for T1D for 14 d. The congenic interval is not drawn to scale.

Table 1. List of polymorphic genes within the Chr. 11 support interval 116.33 to 116.82 Mb

Gene	Position (Mb)*	Protein function	SNPs/Indels†
Qrich2	116.332 to 116.357	Cell adhesion	27/11
Gm11739	116.357 to 116.365	Predicted gene	40/9
Prpsap1	116.361 to 116.385	Nucleotide biosynthesis	31/20
Sphk1	116.422 to 116.428	T-cell trafficking/survival	16/5
Ube2o	116.429 to 116.472	Protein ubiquitination	110/34
Gm11742	116.441 to 116.441	Predicted gene	24/5
Aanat	116.483 to 116.489	Melatonin production	27/11
Rhbdf2	116.489 to 116.518	TNFα secretion	66/21
Cygb	116.536 to 116.545	Oxygen diffusion	1/0
Gm11744	116.545 to 116.559	Predicted gene	4/9
St6galnac2	116.568 to 116.587	Sialic acid transfer	50/13
Gm11735	116.629 to 116.642	Predicted gene	50/10
St6galnac1	116.656 to 116.666	Sialic acid transfer	13/2
Mxra7	116.694 to 116.719	Matrix remodeling	106/33
Jmjd6	116.728 to 116.734	Histone demethylation	29/3
Mettl23	116.734 to 116.741	Mental cognition	14/5
Srsf2	116.741 to 116.745	Thymocyte maturation	10/2
Mfsd11	116.743 to 116.766	Membrane transporter	95/24
Mgat5b	116.810 to 116.878	N-glycan synthesis	60/34

*Marker positions were taken from NCBI build 37.2 (www.ncbi.nlm.nih.gov).
†SNP and Indel types were taken from www.sanger.ac.uk/sanger/Mouse_SnpViewer.
Total number of SNPs and Indels in each candidate gene between the NOD and B6 allele were listed.

NOD allelic variants of individual candidate genes on the same T1D-resistant (NOD× B6.*H2^{g7}*)F1 genetic background (31). The general strategy involved injecting NOD one-cell fertilized embryos with single guide RNA's (sgRNAs) designed to target individual *Idd32* candidate genes (Δ). We then screened for successfully targeted founders containing mutations predicted to disrupt the candidate gene by sequencing the targeted site. Founders with potentially deleterious mutations or reading frame shifts were bred to B6.*H2^{g7}* mice to create F1 progeny where the protective NOD allele was selectively knocked out leaving only the B6 variant intact (NOD.Δ$^{-/-}$ × B6.*H2^{g7}*)F1 (Fig. 5*A*). These mice were tested for T1D after sublethal irradiation and subsequent AI4 T cell injection. We also tested T1D in NOD.*Rag1^{null}* recipients of CD4$^+$ T cells from (NOD.Δ$^{-/-}$ × B6.*H2^{g7}*)F1 knockout progeny cotransferred with AI4 T cells. Standard (NOD× B6.*H2^{g7}*)F1 mice were used as control recipients and CD4$^+$ T cell donors for comparison.

(NOD.Δ$^{-/-}$ x B6.*H2^{g7}*)F1 strains carrying different predicted mutations in *Sphk1*, *Rhbdf2*, and *Ube2o* candidate genes did not develop T1D, ruling them out as contributing to NOD *Idd32*-mediated T1D resistance (Table 2). Next, we interrogated two sialyltransferase encoding genes, *St6galnac1* and *St6galnac2*, which are highly expressed in CD4$^+$ T cells of NOD mice compared to most other inbred mouse strains, including B6 (32). AI4 T cell infusion failed to induce T1D in two different *St6galnac2* F1 mutants, excluding this gene as the causative variant. Next, we tested the T1D susceptibility of 6 different *St6galnac1* F1 mutant strains (strains 1-6) that were created by targeting exon 2 of *St6galnac1*. Surprisingly, strains 1, 2, 3, and 4 were entirely resistant to disease while strains 5 and 6 were susceptible to disease. After comparing the mutation site sequence between T1D-resistant and susceptible strains, we identified that susceptible lines 5 and 6 had a large deletion between *St6galnac1* and *GM11735* (designated as NOD.*St6galnac1-GM11735$^{-/-}$*), an adjacent pseudogene that originated from *St6galnac1*. The altered sequence, a consequence of

the sgRNAs targeting the same exon 2 sequence in both genes, resulted in a hybrid gene in which *St6galnac1* and *GM11735* respectively contributed the 5′ and 3′ segments of exon 2.
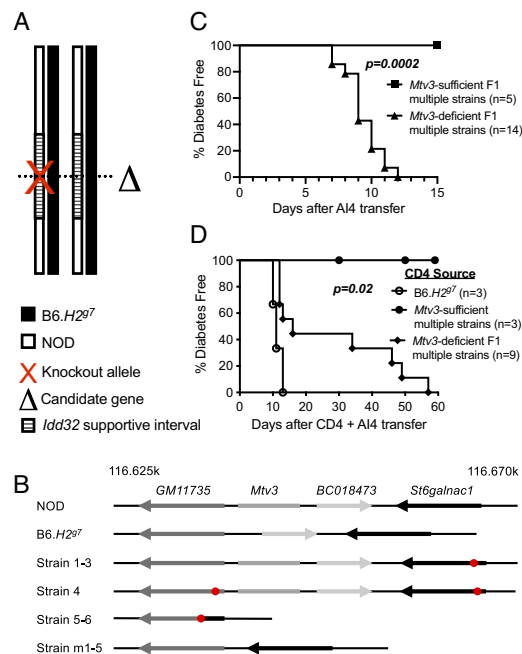

Fig. 5. NOD-encoded *Mtv3* controls susceptibility to CD8$^+$ T cell–induced T1D. (*A*) Schematic illustration of Chr.11 in (NOD × B6.*H2^{g7}*)F1 mice that express both NOD and B6 alleles or only the B6 allele of individual *Idd32* candidate genes. (*B*) Schematic illustration of the *Idd32* locus in NOD and B6.*H2^{g7}* mice as well as NOD strains harboring various mutations of *St6galnac1*, *Gm11735*, and/or *Mtv3*. Red circles indicate CRISPR/Cas9 target sites (described in Table 2). (*C*) T1D incidence in sublethally irradiated B6.*H2^{g7}* mice and multiple *Mtv3*-deficient and *Mtv3*-sufficient F1 mutant strains adoptively transferred with 2 × 10^7 AI4 splenocytes. (*D*) T1D incidence in NOD.*Rag1^{null}* mice adoptively transferred with 2 to 3 × 10^6 CD4$^+$ T cells purified from different *Mtv3*-deficient and -sufficient F1 donors along with 2 × 10^7 AI4 splenocytes. Survival curves were compared by the log-rank test.

Table 2. AI4 CD8⁺ T-cell-induced diabetes in sublethally irradiated (NOD × B6.*H2^{g7}*) F1 mice that express only the B6 allele of different individual candidate genes

Gene	Strain name	Mutation	Fraction diabetic
Sphk1		50 bp deletion	0/7
Sphk1		23 bp insertion	0/5
Sphk1		2 bp insertion	0/3
Rhbdf2		21 bp deletion	0/9
Rhbdf2		2 bp deletion	0/5
Ube2o		78 bp deletion	0/3
St6galnac2		72 bp deletion	0/6
St6galnac2		4 bp deletion	0/5
St6galnac1	Strain 1	65 bp deletion	0/5
St6galnac1	Strain 2	1 bp insertion	0/4
St6galnac1	Strain 3	5 bp deletion	0/8
St6galnac1-GM11735*	Strain 4	2 bp insertion (in each gene)	0/4
St6galnac1-GM11735†	Strain 5	>40 kbp deletion	6/6
St6galnac1-GM11735†	Strain 6	>40 kbp deletion	4/4
Mtv3	Strain m1	>19 kbp deletion	4/4
Mtv3	Strain m2	>19 kbp deletion	3/3
Mtv3	Strain m3	>19 kbp deletion	3/3
Mtv3	Strain m4	>19 kbp deletion	4/4
Mtv3	Strain m5	>19 kbp deletion	1/1

*Strain with deleterious deletions in both *GM11735* and *St6galnac1* without excision of the intervening genomic sequence.
†Strains with a large deletion between exon 2 of *St6galnac1* and exon 2 of *GM11735*.
Recipients were monitored for diabetes development for 15 d after adoptive transfer of 1.5 to 2 × 10⁷ AI4 splenocytes.

We reasoned that our results could be explained by two scenarios: i) that *GM11735*, or both *GM11735* and *St6galnac1*, were the gene(s) underlying *Idd32* or ii) a gene in the intervening region between *GM11735* and *St6galnac1* was the causal variant. Opposing the first scenario, we found that in strain 4, our sgRNAs caused predicted deleterious deletions in both *GM11735* and *St6galnac1* without excision of the intervening genomic sequence. Yet, these mice remained resistant to AI4-mediated T1D. To address the second scenario, we compared the de novo assembled NOD and B6 genome sequences between *GM11735* and *St6galnac1* and found two notable sequences present on the NOD background. The first sequence being a noncoding RNA segment (*BC018473*) with no known functionality, and the second being *Mtv3*, an endogenous retrovirus which has inserted into the NOD genome at this region of Chr. 11 (Fig. 5*B*).

To determine whether *Mtv3* was responsible for NOD *Idd32*-induced T1D resistance, NOD embryos were injected with sgRNAs designed to excise the entire gene as well as the adjacent noncoding RNA segment. Five *Mtv3* knockout founders were produced (Table 2) that were each bred to B6.*H2^{g7}* mice. All F1 progeny from these crosses developed T1D after sublethal irradiation and infusion with AI4 splenocytes (Fig. 5*C*). Furthermore, NOD.*Rag1^{null}* recipients of CD4⁺ T cells from *Mtv3*-deficient F1 mice cotransferred with AI4 splenocytes developed T1D (Fig. 5*D*). These results indicate *Mtv3* as the genetic element underlying *Idd32*.

Mtv3 Deletes Vβ3⁺ CD4⁺ T Cells that Support Pathogenic CD8⁺ T Cell Functions. Previous studies have reported that *Mtv3* encodes a SAg that deletes Vβ3⁺ thymocytes in NOD mice by a mechanism that requires MHC (33, 34). Since CD4⁺ T cells regulate the pathogenic activation of CD8⁺ T cells in T1D, one explanation for our findings is that this Vβ subset is critical for promoting

activation of transferred diabetogenic CD8⁺ T cells in B6.*H2^{g7}* recipient mice. Hence, we originally tested whether ablating *Mtv3* would restore Vβ3⁺ T cell development. The frequency at which individual TCR Vβ is utilized among splenic T cells of NOD and *Mtv3*-deficient NOD.*St6galnac1-GM11735^{-/-}* mice was assessed by staining with anti-TCR Vβ antibodies. T cells bearing Vβ3 represented only 0.4% of NOD CD4⁺ T cells compared to 3.5% of those from NOD.*St6galnac1-GM11735^{-/-}* mice (Fig. 6*A*). Moreover, we found that the level of Vβ3⁺ T cells in *Mtv3*-harboring B6.*H2^{g7}*.*Idd32^{NOD/NOD}* mice was similar to NOD mice. Conversely, standard B6.*H2^{g7}* mice had the same frequency of Vβ3⁺ T cells as our five *Mtv3*-deficient NOD strains (Fig. 6*B*).

To determine whether Vβ3⁺ become preferentially activated during T1D development, we injected NOD.*Rag1^{null}* mice with AI4 T cells combined with CD4⁺ T cells purified from B6.*H2^{g7}*, *Mtv3*-deficient F1, or *Mtv3*-sufficient F1 mice. Vβ3⁺ cells among B6.*H2^{g7}* and *Mtv3*-deficient F1 donor CD4⁺ T cells rapidly increased to high concentrations (>40% of total CD4⁺ T cells). In contrast, the frequency of Vβ3⁺ cells among *Mtv3*-sufficient F1 CD4⁺ T cells did not increase (Fig. 6 *C* and *D*). We also examined Vβ3⁺ CD4⁺ T cells in sublethally irradiated *Mtv3*-deficient and -sufficient F1 mice after NOD.*Rag1^{null}*.*AI4* splenocyte transfer. This found that Vβ3⁺ CD4⁺ T cells become selectively more activated in *Mtv3*-deficient than in *Mtv3*-sufficient F1 mice (Fig. 6*E*).

We next tested whether Vβ3⁺ CD4⁺ T cells were the only Vβ subset involved in pathogenically activating diabetogenic CD8⁺ T cells in our adoptive transfer system. To accomplish this, Vβ3⁺ and Vβ3⁻ CD4⁺ T cells were purified from *Mtv3*-deficient F1 mice and separately cotransferred with NOD.*Rag1^{null}*.*AI4* splenocytes into NOD.*Rag1^{null}* recipients. Only recipients of Vβ3⁺ but not Vβ3⁻ CD4⁺ T cells developed diabetes (Fig. 6*F*). This demonstrates that *Mtv3* controls susceptibility to AI4 T cell–mediated diabetic functions through Vβ3⁺ CD4⁺ T cells alone.
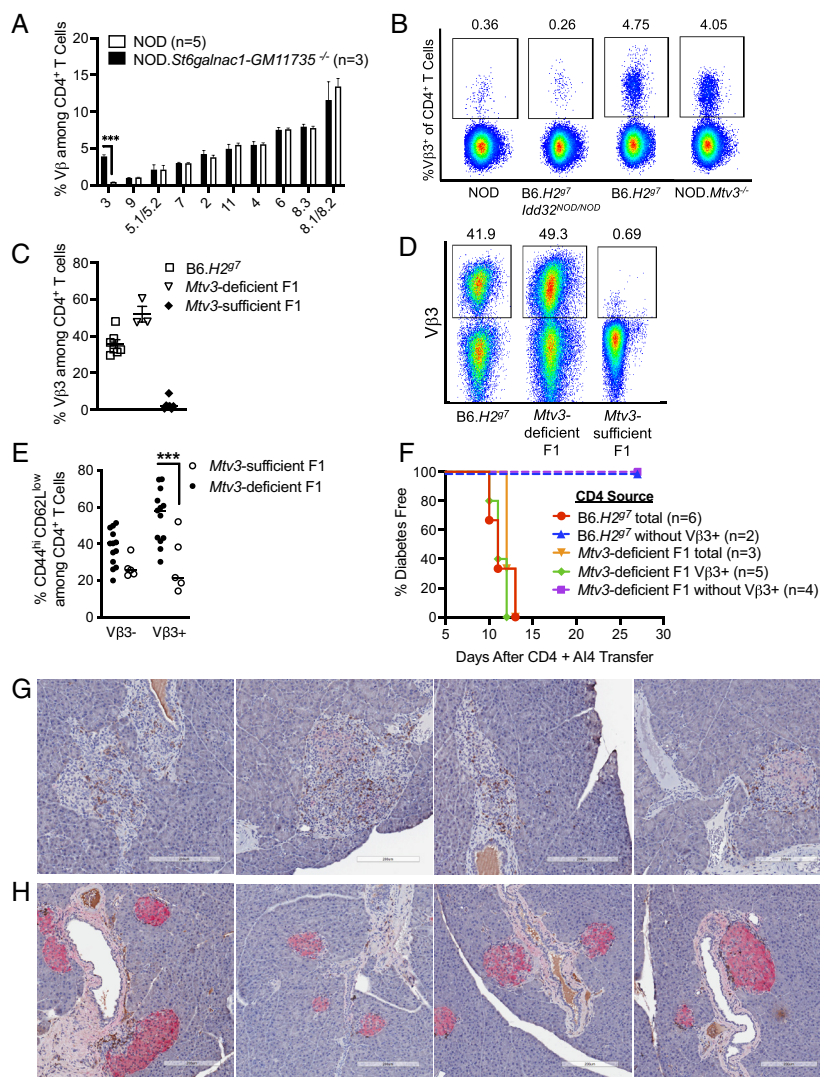
Fig. 6. *Mtv3* inhibits T1D by deleting Vβ3⁺ CD4⁺ T cells that support diabetogenic CD8⁺ T cells. (*A*) The proportion of Vβ subsets based on staining for various TCR Vβ chains among CD4⁺ T cells in spleens of 22-wk-old NOD and NOD.*St6galnac1-GM11735⁻/⁻* mice (strain 6 in Table 2). Results are displayed as mean ± SEM and were analyzed by Bonferroni's multiple comparisons test. ***$P < 0.001$. (*B*) Vβ3⁺ CD4⁺ T cells in spleens of NOD, B6.*H2^{g7}.Idd32^{NOD/NOD}*, B6.*H2^{g7}*, and NOD.*Mtv⁻/⁻* mice. (*C* and *D*) The proportion of Vβ3⁺ T cells among CD4⁺ T cells in spleens of NOD.*Rag1^{null}* mice cotransferred with 2×10^7 AI4 splenocytes and 2 to 3×10^6 purified CD4⁺ T from B6.*H2^{g7}*, *Mtv3*-deficient F1, or *Mtv3*-sufficient F1 mice. (*E*) Frequency of activated (CD44⁺CD62L⁻) Vβ3⁺ and Vβ3⁻ CD4⁺ T cells in splenocytes of sublethally irradiated *Mtv3*-deficient and -sufficient F1 mice from strains m1-m4. Spleens from *Mtv3*-deficient F1 mice were analyzed as they developed T1D between 7- and 13-d post-transfer and *Mtv3*-sufficient F1 mice were analyzed at 15 d post-transfer. (*F*) Incidence of T1D in NOD.*Rag1^{null}* recipients of 2×10^7 AI4 splenocytes cotransferred with 2 to 3×10^6 total or Vβ3-depleted CD4⁺ T cells or 1.5×10^5 purified Vβ3⁺CD4⁺ T cells from *Mtv3*-deficient F1 (strains m3 and m4) or B6.*H2^{g7}* mice. Survival curves were compared by the log-rank test. (*G* and *H*) Immunohistochemistry was used to assess insulitis in NOD.*Rag1^{null}* recipients of 2×10^7 AI4 splenocytes cotransferred with 2×10^6 Vβ3⁺ depleted CD4⁺ T cells or 1.5×10^5 purified Vβ3⁺ CD4⁺ T cells from *Mtv3*-deficient F1 mice. Pancreata were stained for insulin (red) and CD4 (brown). Little insulin staining and widespread infiltration with CD4 staining were observed in pancreata of mice receiving Vβ3⁺ purified CD4⁺ T cells 12 d post-transfer (*G*). Significant insulin staining and little CD4 staining were observed in pancreata of mice receiving Vβ3⁺ depleted CD4⁺ T cells 76 d post-transfer (*H*). Images are longitudinal sections of pancreata at 200× magnification.

To determine whether Vβ3⁺ CD4⁺ T cells directly contribute to beta cell inflammation, CD4⁺ staining was performed on pancreata dissected from NOD.*Rag1^{null}* recipients of Vβ3⁺ or Vβ3⁻ CD4⁺ T cells cotransferred with NOD.*Rag1^{null}.AI4* splenocytes. By 12 d post-transfer, we found substantial numbers of CD4⁺ T cells in the insulitic lesions of Vβ3⁺ CD4⁺ T cell recipients (Fig. 6*G*). In contrast, CD4⁺ staining was negligible in recipients of Vβ3⁻ CD4⁺ T cells, which presented very little insulitis, even at 76 d post-transfer (Fig. 6*H*). Collectively, these results demonstrate that *Mtv3* inhibits autoreactive CD8⁺ T cell functions by deleting Vβ3⁺ CD4⁺ T cells, which harbor a subset of diabetogenic cells that otherwise provide help for pathogenic CD8⁺ T cell activation.

Single-Cell Sequencing Analysis of Mtv3-Reactive Vβ3⁺ CD4⁺ T Cells. To characterize B6.*H2^{g7}* Vβ3⁺ CD4⁺ T cells, which are deleted by NOD-encoded *Mtv3* in B6.*H2^{g7}.Idd32^{NOD/NOD}* mice, paired single-cell RNA sequencing and single-cell TCR sequencing were performed on two separate pools of B6.*H2^{g7}* CD4⁺ T cells 14 d after they were adoptively transferred into two NOD.*Rag1^{null}* recipient mice. A dimensionality reduction analysis of recovered CD4⁺ T cells with a full TCR αβ chain pair revealed 11 distinct clusters by Uniform Manifold Approximation and Projection (UMAP) visualization (Fig. 7*A*). Based on established lineage markers, we identified memory (cluster 0), regulatory (cluster 1), Th1 effector (cluster 2), terminally differentiated (clusters 3),

naïve (cluster 4), cycling (cluster 5), follicular helper (cluster 6), Th17 effector (cluster 8), and cytotoxic (cluster 9) CD4⁺ T cells. Cells in two additional clusters, clusters 7 and 10, did not present well-established CD4⁺ T cell differentiation states; cluster 7 cells displayed a transcriptional profile similar to a population of IL-21⁺ CD4 T cells found in the islets of prediabetic NOD mice (35), while Cluster 10 contained cells with an indistinct phenotype. Development trajectories inferred using the partition-based graph abstraction and RNA velocity combined algorithim predicted that effector/memory T cell subsets emerged from the naïve T cell population and that terminally differentiated CD4⁺ T cells were the most mature subset (Fig. 7*B*). Quantifying the proportion of Vβ3⁺(*Trbv26*⁺) cells in each cluster, we found that *Trbv26*⁺ cells were particularly enriched in the memory and Th1 effector CD4⁺ T cells, as well as cluster 10, while they were relatively scarce among naïve, terminally differentiated, and *Il21* enriched CD4⁺ T cells (Fig. 7 *C* and *D*).

To assess whether Vβ3⁺ CD4⁺ T cell expansion is antigen driven, we analyzed our samples for V(D)J clonotypes and TCR α and β chain gene usage. Both *Trbv26*⁺ and *Trbv26*⁻ cells expressed a similar diversity of Vα and Jα segments indicating that the TCR α chain does not drive Vβ3⁺ T cell expansion (Fig. 7 *E* and *F*). When TCR β CDR3 was separately used to define a clone, we identified 2,695 *Trbv26*⁺ clones, 119 of which were found in both replicates (Dataset S1). Next, we used GLIPH2 to identify
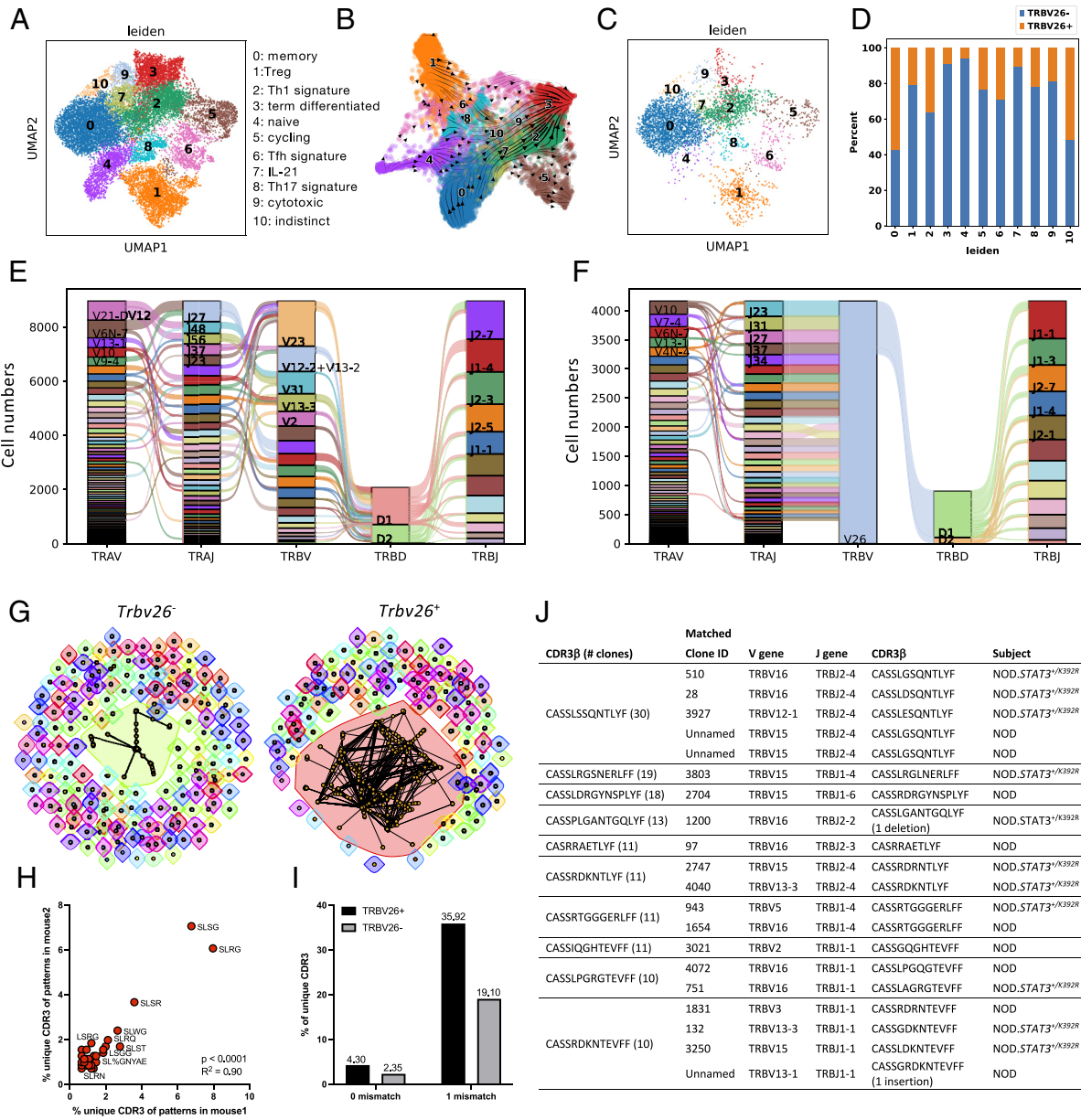
Fig. 7. Single-cell RNA and TCR sequencing analysis of adoptively transferred B6.*H2^{g7}* CD4$^+$ T cells. Two NOD.*Rag1^{null}* mice were injected with separate pools of splenic CD4$^+$ T cells from B6.*H2^{g7}* mice. Recipient spleens were analyzed 14 d after transfer. (*A*) UMAP visualization of CD4$^+$ T cell clusters. (*B*) Distribution of cells according to RNA velocity trajectory inference. (*C*) UMAP plot depicting the distribution of *Trbv26$^+$* cells. (*D*) Proportion of *Trbv26$^+$* and *Trbv26$^-$* cells in each cluster. (*E* and *F*) Sankey plot showing TCRα and β V(D)J gene usage in *Trbv26$^-$* (*E*) and *Trbv26$^+$* (*F*) cells. (*G*) Network analysis of *Trbv26$^+$* and *Trbv26$^-$* CDR3β clusters indicating relationships between TCRs (nodes) that share CDR3β similarity. (*H*) The same local CDR3β motifs were reproduced in TCRs from both donor mice (Dataset S1) with correlated enrichment as determined by the Pearson correlation coefficient. (*I*) Frequency of *Trbv26$^+$* CDR3β sequences with 0 or 1 amino acid mismatch compared to CDR3β sequences from islet infiltrating CD4$^+$ T cells in NOD background mice. Two published datasets were used (36, 37). The same datasets were used to identify islet infiltrating CD4$^+$ T cell clones with 0 or 1 amino acid mismatched CDR3β sequences to our ten most expanded *Trbv26$^+$* clonotypes (*J*).

CDR3β (# clones)	Matched Clone ID	V gene	J gene	CDR3β	Subject	Ref.
CASSLSSQNTLYF (30)	510	TRBV16	TRBJ2-4	CASSLGSQNTLYF	NOD.*STAT3$^{+/K392R}$*	(36)
	28	TRBV16	TRBJ2-4	CASSLDSQNTLYF	NOD.*STAT3$^{+/K392R}$*	(36)
	3927	TRBV12-1	TRBJ2-4	CASSLESQNTLYF	NOD.*STAT3$^{+/K392R}$*	(36)
	Unnamed	TRBV15	TRBJ2-4	CASSLGSQNTLYF	NOD	(37)
	Unnamed	TRBV15	TRBJ2-4	CASSLGSQNTLYF	NOD	(37)
CASSLRGSNERLFF (19)	3803	TRBV15	TRBJ1-4	CASSLRGLNERLFF	NOD.*STAT3$^{+/K392R}$*	(36)
CASSLDRGYNSPLYF (18)	2704	TRBV15	TRBJ1-6	CASSRDRGYNSPLYF	NOD	(36)
CASSPLGANTGQLYF (13)	1200	TRBV16	TRBJ2-2	CASSLGANTGQLYF (1 deletion)	NOD.STAT3$^{+/K392R}$	(36)
CASRRAETLYF (11)	97	TRBV16	TRBJ2-3	CASRRAETLYF	NOD	(36)
CASSRDKNTLYF (11)	2747	TRBV15	TRBJ2-4	CASSRDRNTLYF	NOD.*STAT3$^{+/K392R}$*	(36)
	4040	TRBV13-3	TRBJ2-4	CASSRDKNTLYF	NOD.*STAT3$^{+/K392R}$*	(36)
CASSRTGGGERLFF (11)	943	TRBV5	TRBJ1-4	CASSRTGGGERLFF	NOD.*STAT3$^{+/K392R}$*	(36)
	1654	TRBV16	TRBJ1-4	CASSRTGGGERLFF	NOD	(36)
CASSIQGHTEVFF (11)	3021	TRBV2	TRBJ1-1	CASSGQGHTEVFF	NOD	(36)
CASSLPGRGTEVFF (10)	4072	TRBV16	TRBJ1-1	CASSLPGQGTEVFF	NOD	(36)
	751	TRBV16	TRBJ1-1	CASSLAGRGTEVFF	NOD.*STAT3$^{+/K392R}$*	(36)
CASSRDKNTEVFF (10)	1831	TRBV3	TRBJ1-1	CASSRDRNTEVFF	NOD	(36)
	132	TRBV13-3	TRBJ1-1	CASSGDKNTEVFF	NOD.*STAT3$^{+/K392R}$*	(36)
	3250	TRBV15	TRBJ1-1	CASSLDKNTEVFF	NOD.*STAT3$^{+/K392R}$*	(36)
	Unnamed	TRBV13-1	TRBJ1-1	CASSGRDKNTEVFF (1 insertion)	NOD	(37)

specificity groups within the *Trbv26$^+$* CDR3β repertoire. This package clusters TCRs with a high probability of sharing antigen specificity due to both conserved motifs (motifs >10 fold enriched, 0.001 > probability of enrichment by chance) and global similarity (CDR3s differing by up to one amino acid) of CDR3 sequences (38). This involves selecting CDR3β sequences with statistically significant motifs compared to a reference set of CDR3β sequences (Fisher_score < 0.05). We found that a high proportion Vβ3$^+$ TCR sequences fell within a single cluster of related CDR3β sequences (Fig. 7*G*). These were composed of 29 enriched CDR3 4mer motif patterns (Fig. 7*H*) as well as several globally conserved CDR3 sequences (each pattern containing > 5 unique CDR3s), the most prominent of which arose from Vβ3/Jβ1.1 pairings (Dataset S2).

To investigate whether our *Trbv26$^+$* sequences could be linked to previously identified islet-reactive TCR β chains, we aligned our *Trbv26$^+$* sequences to 10,900 CDR3β sequences from two studies that performed single-cell TCR sequencing on T cells from NOD background mice. One study analyzed islet infiltrating T cells in mutant NOD mice carrying a human gain of function mutation in STAT3 (NOD.*STAT3$^{+/K392R}$*) that substantially accelerates T1D onset compared to standard NOD mice (36). The second study analyzed insulin-specific CD4$^+$ T cells during the early prediabetic phase of disease in PLN and islets of NOD mice (37). Against these two datasets, we identified 116 exact CDR3β matches (4.3%) and 968 matches within one amino acid mismatch (36%) for CDRs of the same length, which was considerably higher in
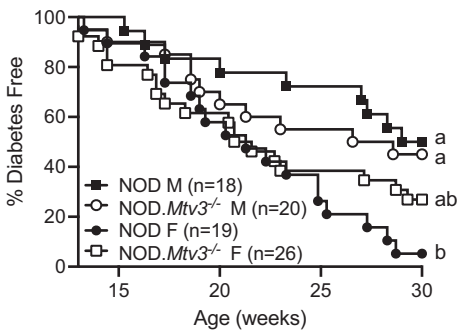
Fig. 8. Spontaneous T1D in wild-type NOD vs. *Mtv3*-deficient NOD mice. The incidence of T1D in male and female mice of the indicated genotypes. Combined data from four NOD.*Mtv3*$^{-/-}$ strains (m2, m3, m4, and m5 in Table 2) are shown. Survival curves with no common letters differ significantly ($P < 0.05$) when compared by the log-rank test.

proportion compared to *Trbv26*$^-$ clonotypes that harbor all the remaining Vβ segments (Fig. 7*I*). These CDR3βs (either exact matches or 1 mismatch) were found for our 10 most expanded *Trbv26*$^+$ CDR3β sequences, the majority of which were from the islet infiltrate of NOD. *STAT*$^{+/K392R}$ mice (Fig. 7*J*). Our most dominant *Trbv26*$^+$ CDR3β sequence, CASSLSSQNTLYF, included matches for two insulin peptide MHC tetramer reactive clones that used Vβ15/Jβ24 pairings. Interestingly, almost identical sequences (CASSLGSQNTLYF and CASSLGGQNTLYF) from a Vβ15/Jβ2.4 pairing were reported in a study of CDRs of public memory CD4$^+$ T cell clonotypes isolated from PLN of prediabetic and diabetic NOD mice (39). These findings suggest that Mtv3-reactive Vβ3$^+$ CD4$^+$ T cells in B6.*H2*^{g7} mice include clonotypes capable of recognizing the same islet antigen(s) as a subpopulation of autoreactive CD4$^+$ T cells in NOD mice.

Unaltered Spontaneous T1D Presentation in Mtv3-Deficient NOD Mice. Finally, we tested whether deleting *Mtv3* and restoring Vβ3$^+$ T cells would affect spontaneous T1D in NOD mice. The timing of onset and the incidence of disease were similar between NOD and *Mtv3*-deficient NOD (NOD.*Mtv3*$^{-/-}$) mice, indicating that diabetes presentation in NOD mice is unaltered by *Mtv3*-mediated depletion of Vβ3$^+$ T cells (Fig. 8).

Discussion

It has been known for decades that most common inbred mouse strains carry between 2 and 8 endogenous *Mtvs*, all of which express functional SAgs that create gaps in the peripheral T cell repertoire through intrathymic deletion of cognate T cells (40). However, the importance of this phenomenon for mouse models of autoimmune diseases has not been determined. Here, we report that the *Mtv3* provirus harbored by NOD mice deletes Vβ3$^+$ CD4$^+$ T cells that includes a population of SAg-reactive T cells which in some contexts can contribute to T1D pathogenesis. This work establishes *Mtv3* SAg as the dominantly protective genetic element underlying our previously identified *Idd32* locus (25). This represents one of several loci where the NOD allele paradoxically confers T1D resistance (1, 41). The protective effect of such intervals is usually masked by the large number of T1D susceptibility genes carried by this strain but can be revealed in outcrosses of NOD mice to other strains. It is notable that *Idd32* is the only *Idd* locus discovered thus far where the underlying gene is an endogenous retrovirus.

Mtv3 SAg-reactive CD4$^+$ T cells appear to recognize a beta cell antigen(s) since Vβ3$^+$ CD4$^+$ T cells purified from *Mtv3* deficient NOD mice accumulated in islet infiltrates after adoptive transfer.

This is consistent with a previous finding that although Vβ3$^+$ T cells are very rare in NOD mice, the small number which survive intrathymic deletion make up a high proportion of those in the earliest islet infiltrates (42). Interestingly, circulating Vβ3$^+$ T cells in this strain present an activated phenotype which may be because those escaping clonal deletion become pathogenically activated from SAg presentation by peripheral APCs (43). In our model system, Vβ3$^+$ T cells were not the final effectors of beta cell destruction. Instead, they precipitated T1D through pathogenically activating diabetogenic CD8$^+$ T cells which in turn kill beta cells through their cytotoxic effector functions. Apart from a requirement for CD40-CD40L interactions, the precise nature of this CD4$^+$ T cell help remains undetermined. However, it is likely to involve DC licensing and/or the production of T helper cytokines, which are mechanisms through which CD4$^+$ T cells are known to support pathogenic CD8$^+$ T cells in NOD mice (44). We found that our AI4/CD4$^+$ T cell coadoptive transfer system induced T1D with equal efficiency in Rag1-deficient NOD and B6.*H2*^{g7} recipients. This indicates that the diabetogenic capacity of Vβ3$^+$ CD4$^+$ T cells is not influenced by *Mtv3* SAg presentation by peripheral APCs after adoptive transfer. The CDR3β clustering pattern we observed in proliferated B6.*H2*^{g7} Vβ3$^+$ CD4$^+$ T cells in adoptively transferred NOD.*Rag1*^{null} hosts is indicative of antigen-driven clonal expansion. Among these clonotypes, we identified numerous CDR3β sequences also found in CD4$^+$ T cells from islet infiltrates and PLN of NOD mice (36, 37). Since it is rare that T cells with unrelated antigen specificities share CDR sequences, this finding suggests that B6.*H2*^{g7} Vβ3$^+$ CD4$^+$ T cells harbor clonotypes capable of recognizing the same islet antigen(s) as a portion of CD4$^+$ T cells in NOD mice. In the future, it would be interesting to determine whether *Mtv3*-reactive Vβ3$^+$ CD4$^+$ T cells respond to any of the currently known diabetes-related autoantigens.

While it is not specifically demonstrated that *Mtv* SAgs play a direct role in an autoimmune process, previous work has demonstrated that these molecules modulate immune responses in experimental murine models of cancer and infectious disease (40). In models of polyomavirus- and Esb-induced lymphoma, the presence of the *Mtv7* SAg presents a selective disadvantage by eliminating a population of T cells that are critical for tumor immunity (45–47). On the other hand, SAgs from *Mtv7* and *Mtv29* activate T cells respectively required to support the development of neuropathogenesis during *Plasmodium berghei* ANKA infection and spontaneous B cell lymphomagenesis (48–50). It was possible to detect the involvement of *Mtv* SAgs in these disorders because they delete or activate a single critical TCR Vβ specificity that recognizes a discrete MHC-restricted antigen, such as an immunodominant peptide derived from the PyV middle T protein (51) and *Mtv7*-encoded SAgs for Esb and B cell lymphomagenesis (47). In contrast, there is little evidence to support a role for *Mtv* SAgs in mouse models of complex diseases where pathology can be driven by T cells bearing different combinations of Vβ specificities. Indeed, we found that deleting *Mtv3* and restoring Vβ3$^+$ T cells in NOD mice did not affect their susceptibility to spontaneous T1D. This is not surprising given that almost half of murine Vβ gene segments are dispensable for disease in this model (52). Such redundancy is strikingly divergent from the adoptively transferred CD8$^+$ T cell–mediated T1D we observed in B6.*H2*^{g7} mice, which is under the control of a single CD4$^+$ TCR Vβ segment. This binary presentation of disease resembles T1D in rat strains bearing the high-risk MHC II haplotype RT1.B/D^u, which is controlled by a single CD4$^+$ TCR Vβ specificity, Vβ13 (53). The TCR Vβ13 encoding gene segment is harbored within a dominant rat diabetes susceptibility locus (*Iddm14*) (54–56). The *TcrbV13S1A1* allele is expressed by six T1D susceptible rat strains, whereas strains that are resistant express either *TcrbV13S1A2* or a nonfunctional

version of the gene (*TcrbV13S1A3P*). Selective antibody depletion or genetic deletion of Vβ13⁺ T cells prevents disease in the susceptible rat strains (57, 58). Like *Mtv3*, this is an example of a genome-encoded element (polymorphisms in the TCR-Vβ13 gene) that controls T1D susceptibility by altering the TCR repertoire.

Although HERVs are associated with a variety of autoimmune disorders, including T1D (4, 59, 60), it is largely unknown whether humans harbor retroviral SAgs with potential for Vβ-specific T cell deletion/activation. HERVs account for ~9% of the genome and some families, including HERV-K(C4), HERV-K10, and HERV-K18, are closely related in sequence similarity to *Mtvs* (8, 61–63). Previous studies have described an HERV-K18 family-related endogenous retroviral sequence, designated IDDMK(1,2)22, encoding a protein with SAg properties in T1D patients (7, 8). Membrane expression of this SAg was thought to account for the preferential expansion of Vβ7⁺ T cells found in the insulitic lesions of patients at the clinical onset of T1D. However, virus expression was later attributed to DNA contamination in PCR-amplified sequences (10, 11, 64, 65). Another study showed that the HERV-K18 envelope gene on human Chr. 1 encodes an SAg capable of inducing the negative thymic selection of Vβ7⁺ CD4⁺ T cells in an in vitro assay (14). Separately, polymorphisms in the HERV-K18 SAg were reported to be associated with T1D risk (6). However, this was later refuted (9). A low number of HERV-K copies in the complement component C4 (C4) gene cluster has been associated with T1D risk (13). C4 is the second gene in the four-gene RCCX cassette located midway between MHC class I and class II genes and is highly variable for copy number and HERV-K(C4) inclusion (66). Having zero or one copy of HERV-K(C4) has been associated with T1D susceptibility independently of the linkage between HERV-K(C4) and the MHC class II interval (13). It is tempting to speculate that HERV-K(C4) encodes a SAg that deletes TCR specificities that are important for human T1D development, analogous to *Mtv3*. However, the challenge with identifying such SAg–T cell interactions in genetically heterogeneous humans is that different MHC II alleles exhibit strikingly dissimilar SAg presentation abilities (67–69). Nevertheless, the possibility that the human genome encodes SAgs capable of influencing disease when expressed in genetically susceptible individuals is intriguing and deserves further study.

Finally, our work raises interesting questions about the impact of *Mtvs* on mouse models of human immune responses. *Mtv* SAgs are thought to be retained to protect against the horizontal transmission of exogenous milk-borne MMTV infections as these viruses are lymphotrophic and rely on SAg-induced T cell activation in their life cycle (70). However, given that i) *Mtvs* harbored by common mouse strains affect a high proportion of Vβ families, ii) both CD4⁺ and CD8⁺ T cell are subject to deletion by SAgs, and iii) most inbred mouse strains inherit between 2 and 8 *Mtvs* (17, 40), it seems likely that *Mtv* SAgs have more of an influence on mouse models of human immune responses than we currently realize. Dissecting such complexity presents a difficult task, which in most cases the relevancy for the human disease being modeled remains unclear. Hence, in the future, it may be desirable to study human immune responses using stocks of *Mtv* knockout mice that express a full Vβ TCR repertoire, which could easily be generated using existing gene-editing technologies. At the same time, further study of *Mtv* SAgs remains a worthwhile endeavor as their interactions with the immune system offer unique insights into a host of human pathologies, including cancers, infectious diseases, and autoimmunity. A good example is the current work in which

transferring *Mtv3* to normally spontaneous T1D-resistant B6.*H2^{g7}* mice revealed a population of diabetogenic CD4⁺ T cells that may recognize an autoantigen of importance for human T1D.

Although our current study provides proof of principle that retroviral SAgs can contribute to T1D pathogenesis, it is unresolved whether humans harbor retroviral SAgs with potential for Vβ-specific T cell deletion/activation. However, given that HERVs account for a significant portion of the human genome, that some human retrovirus families are closely related in sequence similarity to *Mtvs*, and that HERVs are associated with a variety of autoimmune disorders, including T1D, this question deserves revisiting. Another consideration is that we used an adoptive transfer model of T1D which is considered somewhat artificial compared to the spontaneous form of T1D that arises in NOD mice. However, our platform provides unique opportunities to detect gene-masking and gene-gene interaction effects that are normally concealed or absent in NOD mice, which may be of importance for certain subtypes of the human disease. A good example is *Mtv3* that has no detectable impact in NOD mice but is highly protective against T1D in B6 background mice.

Methods and Methods

An extended description of mouse strains, genetic analysis, adoptive transfer studies, flow cytometry, immunohistochemistry, single-cell RNA and TCR sequencing, and additional data that contribute to the results are provided in *SI Appendix*. In brief, we generated a congenic stock of B6.*H2^{g7}* mice homozygous for the NOD allele of *Idd32* and confirmed its resistance to CD8⁺ T cell–induced T1D. Subsequent adoptive transfer studies using *Rag1*-deficient B6.*H2^{g7}* or NOD mice as hosts showed that the effect is manifested through CD4⁺ T cells. Next, we shortened the *Idd32* congenic interval by generating 9 B6.*H2^{g7}* subcongenic stocks expressing different NOD-derived segments of the original *Idd32* interval and tested them for CD8⁺ T cell–mediated T1D susceptibility. Candidate genes in the shortened *Idd32* region were assessed using a CRISPR/Cas9 screen designed for the selective expression of only the B6 or both the B6 and NOD allelic variants of individual candidate genes on the same T1D-resistant (NODx B6.*H2^{g7}*)F1 genetic background. We tested several (NODx B6.*H2^{g7}*)F1 mutant mice for T1D susceptibility which identified *Mtv3* as the likely candidate for *Idd32*. This was confirmed by demonstrating the susceptibility to CD8⁺ T cell–induced T1D of (NODx B6.*H2^{g7}*)F1 mice from which *Mtv3* was excised. Additional adoptive transfer studies were performed to show that *Mtv3* confers T1D resistance by deleting Vβ3⁺ CD4⁺ T cells, which otherwise accumulate in insulitic lesions and trigger the pathogenic activation of diabetogenic CD8⁺ T cells in B6 background mice. We also performed paired single-cell TCR sequencing and single-cell RNA sequencing to document that Vβ3⁺ CD4⁺ T cell activation is likely antigen driven. Last, we performed a T1D incidence study to assess whether deleting *Mtv3* and restoring Vβ3⁺ T cells would affect spontaneous T1D development in NOD mice.

Author affiliations: [a]Department of Animal Sciences, University of Florida, Gainesville, FL 32611; [b]Division of Animal Sciences, University of Missouri, Columbia, MO 65201; [c]Department of Physiology, Medical College of Wisconsin, Milwaukee, WI 53226; [d]Department of Pathology, Immunology and Laboratory Medicine, University of Florida, Gainesville, FL 32610; [e]The Jackson Laboratory, Bar Harbor, ME 04609; and [f]Department of Pediatrics, Medical College of Wisconsin, Milwaukee, WI 53226

1. J. P. Driver, Y. G. Chen, C. E. Mathews, Comparative genetics: Synergizing human and NOD mouse studies for identifying genetic causation of type 1 diabetes. *Rev. Diabet. Stud.* **9**, 169–187 (2012).
2. A. Pugliese, Autoreactive T cells in type 1 diabetes. *J. Clin. Invest.* **127**, 2881–2891 (2017).
3. A. W. Purcell, S. Sechi, T. P. DiLorenzo, The evolving landscape of autoantigen discovery and characterization in type 1 diabetes. *Diabetes* **68**, 879–886 (2019).
4. S. Levet *et al.*, Human endogenous retroviruses and type 1 diabetes. *Curr. Diab. Rep.* **19**, 141 (2019).
5. M. McDuffie, A. Ostrowska, Superantigen-like effects and incidence of diabetes in NOD mice. *Diabetes* **42**, 1094–1098 (1993).
6. S. Marguerat, W. Y. Wang, J. A. Todd, B. Conrad, Association of human endogenous retrovirus K-18 polymorphisms with type 1 diabetes. *Diabetes* **53**, 852–854 (2004).
7. B. Conrad *et al.*, Evidence for superantigen involvement in insulin-dependent diabetes mellitus aetiology. *Nature* **371**, 351–355 (1994).
8. B. Conrad *et al.*, A human endogenous retroviral superantigen as candidate autoimmune gene in type 1 diabetes. *Cell* **90**, 303–313 (1997).
9. E. Ramos-Lopez *et al.*, Neither an intronic CA repeat within the CD48 gene nor the HERV-K18 polymorphisms are associated with type 1 diabetes. *Tissue Antigens* **68**, 147–152 (2006).
10. E. Jaeckel *et al.*, No evidence for association between IDDMK(1,2)22, a novel isolated retrovirus, and IDDM. *Diabetes* **48**, 209–214 (1999).
11. A. Muir, Q. G. Ruan, M. P. Marron, J. X. She, The IDDMK(1,2)22 retrovirus is not detectable in either mRNA or genomic DNA from patients with type 1 diabetes. *Diabetes* **48**, 219–222 (1999).
12. S. Levet *et al.*, An ancestral retroviral protein identified as a therapeutic target in type-1 diabetes. *JCI Insight* **2**, e94387 (2017).
13. M. J. Mason *et al.*, Low HERV-K(C4) copy number is associated with type 1 diabetes. *Diabetes* **63**, 1789–1795 (2014).
14. F. Meylan *et al.*, Negative thymocyte selection to HERV-K18 superantigens in humans. *Blood* **105**, 4377–4382 (2005).
15. R. B. Jones *et al.*, HERV-K-specific T cells eliminate diverse HIV-1/2 and SIV primary isolates. *J. Clin. Invest.* **122**, 4473–4489 (2012).
16. B. Charvet *et al.*, SARS-CoV-2 awakens ancient retroviral genes and the expression of proinflammatory HERV-W envelope protein in COVID-19 patients. *iScience* **26**, 106604 (2023).
17. M. T. Scherer, L. Ignatowicz, A. Pullen, J. Kappler, P. Marrack, The use of mammary tumor virus (Mtv)-negative and single-Mtv mice to evaluate the effects of endogenous viral superantigens on the T cell repertoire. *J. Exp. Med.* **182**, 1493–1504 (1995).
18. S. Ghosh *et al.*, Polygenic control of autoimmune diabetes in nonobese diabetic mice. *Nat. Genet.* **4**, 404–409 (1993).
19. M. A. McAleer *et al.*, Crosses of NOD mice with the related NON strain. A polygenic model for IDDM. *Diabetes* **44**, 1186–1195 (1995).
20. K. R. Simpfendorfer, R. A. Strugnell, T. C. Brodnicki, O. L. Wijburg, Increased autoimmune diabetes in pIgR-deficient NOD mice is due to a "Hitchhiking" interval that refines the genetic effect of Idd5.4. *PLoS One* **10**, e0121979 (2015).
21. K. Hunter *et al.*, Interactions between Idd5.1/Ctla4 and other type 1 diabetes genes. *J. Immunol.* **179**, 8341–8349 (2007).
22. H. I. Fraser *et al.*, Ptpn22 and Cd2 variations are associated with altered protein expression and susceptibility to type 1 diabetes in nonobese diabetic mice. *J. Immunol.* **195**, 4841–4852 (2015).
23. U. C. Rogner, C. Boitard, J. Morin, E. Melanitou, P. Avner, Three loci on mouse chromosome 6 influence onset and final incidence of type I diabetes in NOD.C3H congenic strains. *Genomics* **74**, 163–171 (2001).
24. J. E. Hollis-Moffatt, S. M. Hook, T. R. Merriman, Colocalization of mouse autoimmune diabetes loci Idd21.1 and Idd21.2 with IDDM6 (human) and Iddm3 (rat). *Diabetes* **54**, 2820–2825 (2005).
25. J. P. Driver, Y. G. Chen, W. Zhang, S. Asrat, D. V. Serreze, Unmasking genes in a type 1 diabetes-resistant mouse strain that enhances pathogenic CD8 T-cell responses. *Diabetes* **60**, 1354–1359 (2011).
26. Y. Choi, P. Marrack, J. W. Kappler, Structural analysis of a mouse mammary tumor virus superantigen. *J. Exp. Med.* **175**, 847–852 (1992).
27. A. J. Korman, P. Bourgarel, T. Meo, G. E. Rieckhof, The mouse mammary tumour virus long terminal repeat encodes a type II transmembrane glycoprotein. *EMBO J.* **11**, 1901–1905 (1992).
28. K. Yazdanbakhsh, C. G. Park, G. M. Winslow, Y. Choi, Direct evidence for the role of COOH terminus of mouse mammary tumor virus superantigen in determining T cell receptor V beta specificity. *J. Exp. Med.* **178**, 737–741 (1993).
29. H. Acha-Orbea *et al.*, Clonal deletion of V beta 14-bearing T cells in mice transgenic for mammary tumour virus. *Nature* **350**, 207–211 (1991).
30. D. Lamont *et al.*, Compensatory mechanisms allow undersized anchor-deficient class I MHC ligands to mediate pathogenic autoreactive T cell responses. *J. Immunol.* **193**, 2135–2146 (2014).
31. M. H. Presley, B. Foda, D. V. Serreze, Y. G. Chen, Combined congenic mapping and nuclease-based gene targeting for studying allele-specific effects of Tnfrsf9 within the Idd9.3 autoimmune diabetes locus. *Sci. Rep.* **9**, 4316 (2019).
32. S. Mostafavi *et al.*, Variation and genetic control of gene expression in primary immunocytes across inbred mouse strains. *J. Immunol.* **193**, 4485–4496 (2014).
33. S. Fairchild, A. M. Knight, P. J. Dyson, K. Tomonari, Co-segregation of a gene encoding a deletion ligand for Tcrb-V3+ T cells with Mtv-3. *Immunogenetics* **34**, 227–230 (1991).
34. M. McDuffie *et al.*, I-E-independent deletion of V beta 17a+ T cells by Mtv-3 from the nonobese diabetic mouse. *J. Immunol.* **148**, 2097–2102 (1992).
35. A. E. Ciecko *et al.*, Heterogeneity of Islet-Infiltrating IL-21+ CD4 T Cells in a Mouse Model of Type 1 Diabetes. *J. Immunol.* **210**, 935–946 (2023).
36. J. T. Warshauer *et al.*, A human mutation in STAT3 promotes type 1 diabetes through a defect in CD8+ T cell tolerance. *J. Exp. Med.* **218**, e20210759 (2021).
37. L. Gioia *et al.*, Position β57 of I-A^{g7} controls the early anti-insulin response and onset of diabetes in NOD mice to link MHC and disease. *Sci. Immunol.* **4**, eaaw6329 (2019).
38. H. Huang, C. Wang, F. Rubelt, T. J. Scriba, M. M. Davis, Analyzing the *Mycobacterium tuberculosis* immune response by T-cell receptor clustering with GLIPH2 and genome-wide antigen screening. *Nat. Biotechnol.* **38**, 1194–1202 (2020).
39. I. Marrero, C. Aguilera, D. E. Hamm, A. Quinn, V. Kumar, High-throughput sequencing reveals restricted TCR Vβ usage and public TCRβ clonotypes among pancreatic lymph node memory CD4(+) T cells and their involvement in autoimmune diabetes *Mol. Immunol.* **74**, 82–95 (2016).
40. M. P. Holt, E. M. Shevach, G. A. Punkosdy, Endogenous mouse mammary tumor viruses (mtv): New roles for an old virus in cancer, infection, and immunity. *Front. Oncol.* **3**, 287 (2013).
41. Y. G. Chen, C. E. Mathews, J. P. Driver, The role of NOD mice in type 1 diabetes research: Lessons from the past and recommendations for the future. *Front. Endocrinol. (Lausanne)* **9**, 51 (2018).
42. K. A. Galley, J. S. Danska, Peri-islet infiltrates of young non-obese diabetic mice display restricted TCR beta-chain diversity. *J. Immunol.* **154**, 2969–2982 (1995).
43. P. P. Chiu, A. M. Jevnikar, J. S. Danska, Genetic control of T and B lymphocyte activation in nonobese diabetic mice. *J. Immunol.* **167**, 7169–7179 (2001).
44. L. S. Walker, M. von Herrath, CD4 T cell differentiation in type 1 diabetes. *Clin. Exp. Immunol.* **183**, 16–29 (2016).
45. A. E. Lukacher *et al.*, Susceptibility to tumors induced by polyoma virus is conferred by an endogenous mouse mammary tumor virus superantigen. *J. Exp. Med.* **181**, 1683–1692 (1995).
46. V. Schirrmacher *et al.*, Loss of endogenous mouse mammary tumor virus superantigen increases tumor resistance. *J. Immunol.* **161**, 563–570 (1998).
47. V. Schirrmacher, S. Müerköster, M. Bucur, V. Umansky, M. Rocha, Breaking tolerance to a tumor-associated viral superantigen as a basis for graft-versus-leukemia reactivity. *Int. J. Cancer* **87**, 695–706 (2000).
48. M. I. Boubou *et al.*, T cell response in malaria pathogenesis: Selective increase in T cells carrying the TCR V(beta)8 during experimental cerebral malaria. *Int. Immunol.* **11**, 1553–1562 (1999).
49. O. Gorgette *et al.*, Deletion of T cells bearing the V beta8.1 T-cell receptor following mouse mammary tumor virus 7 integration confers resistance to murine cerebral malaria. *Infect Immun.* **70**, 3701–3706 (2002).
50. N. Sen *et al.*, META-controlled env-initiated transcripts encoding superantigens of murine Mtv29 and Mtv7 and their possible role in B cell lymphomagenesis. *J. Immunol.* **166**, 5422–5429 (2001).
51. A. E. Lukacher, C. S. Wilson, Resistance to polyoma virus-induced tumors correlates with CTL recognition of an immunodominant H-2Dk-restricted epitope in the middle T protein. *J. Immunol.* **160**, 1724–1734 (1998).
52. J. A. Shizuru, C. Taylor-Edwards, A. Livingstone, C. G. Fathman, Genetic dissection of T cell receptor V beta gene requirements for spontaneous murine diabetes. *J. Exp. Med.* **174**, 633–638 (1991).
53. R. A. Eberwine, L. Cort, M. Habib, J. P. Mordes, E. P. Blankenhorn, Autoantigen-induced focusing of Vβ13+ T cells precedes onset of autoimmune diabetes in the LEW.1WR1 rat *Diabetes* **63**, 596–604 (2014).
54. E. P. Blankenhorn *et al.*, The rat diabetes susceptibility locus Iddm4 and at least one additional gene are required for autoimmune diabetes induced by viral infection. *Diabetes* **54**, 1233–1237 (2005).
55. E. P. Blankenhorn, L. Cort, D. L. Greiner, D. L. Guberski, J. P. Mordes, Virus-induced autoimmune diabetes in the LEW.1WR1 rat requires Iddm14 and a genetic locus proximal to the major histocompatibility complex. *Diabetes* **58**, 2930–2938 (2009).
56. J. P. Mordes *et al.*, The iddm4 locus segregates with diabetes susceptibility in congenic WF.iddm4 rats. *Diabetes* **51**, 3254–3262 (2002).
57. J. P. Mordes *et al.*, Analysis of the rat Iddm14 diabetes susceptibility locus in multiple rat strains: Identification of a susceptibility haplotype in the Tcrb-V locus. *Mamm Genome* **20**, 162–169 (2009).
58. J. P. Mordes *et al.*, T cell receptor genotype and Ubash3a determine susceptibility to rat autoimmune diabetes. *Genes (Basel)* **12**, 852 (2021).
59. N. Grandi, E. Tramontano, Human endogenous retroviruses are ancient acquired elements still shaping innate immune responses. *Front. Immunol.* **9**, 2039 (2018).
60. I. Posso-Osorio, G. J. Tobón, C. A. Cañas, Human endogenous retroviruses (HERV) and non-HERV viruses incorporated into the human genome and their role in the development of autoimmune diseases. *J. Transl. Autoimmun.* **4**, 100137 (2021).
61. M. Ono, Molecular biology of type A endogenous retrovirus. *Kitasato Arch. Exp. Med.* **63**, 77–90 (1990).
62. G. C. Franklin *et al.*, Expression of human sequences related to those of mouse mammary tumor virus. *J. Virol.* **62**, 1203–1210 (1988).
63. M. Ono, T. Yasunaga, T. Miyata, H. Ushikubo, Nucleotide sequence of human endogenous retrovirus genome related to the mouse mammary tumor virus genome. *J. Virol.* **60**, 589–598 (1986).
64. V. J. Murphy *et al.*, Retroviral superantigens and type 1 diabetes mellitus. *Cell* **95**, 9–11, discussion 16 (1998).
65. A. Kim *et al.*, Human endogenous retrovirus with a high genomic sequence homology with IDDMK(1,2)22 is not specific for Type I (insulin-dependent) diabetic patients but ubiquitous. *Diabetologia* **42**, 413–418 (1999).
66. M. Tassabehji *et al.*, Identification of a novel family of human endogenous retroviruses and characterization of one family member, HERV-K(C4), located in the complement C4 gene cluster. *Nucleic Acids Res.* **22**, 5211–5217 (1994).
67. M. Kotb *et al.*, An immunogenetic and molecular basis for differences in outcomes of invasive group A streptococcal infections. *Nat. Med.* **8**, 1398–1404 (2002).
68. G. Rajagopalan *et al.*, Evaluating the role of HLA-DQ polymorphisms on immune response to bacterial superantigens using transgenic mice. *Tissue Antigens* **71**, 135–145 (2008).
69. M. Llewelyn *et al.*, HLA class II polymorphisms determine responses to bacterial superantigens. *J. Immunol.* **172**, 1719–1726 (2004).
70. T. V. Golovkina, A. Chervonsky, J. P. Dudley, S. R. Ross, Transgenic mouse mammary tumor virus superantigen expression prevents viral infection. *Cell* **69**, 637–645 (1992).
71. J. P. Driver, W. Gu, Single cell sequencing analysis of adoptively transferred CD4+ T-cells from B6.NOD-(D17Mit21-D17Mit10)/LtJ mice. NCBI GEO. https://www.ncbi.nlm.nih.gov/geo/query/acc.cgi?acc=GSE233060. Deposited 11 October 2023.
72. J. P. Driver, W. Gu, mouse_tcr. Github. https://github.com/Driver-lab1/mouse_tcr. Deposited 6 June 2023.